ENVIRONMENTAL SCIENCES

Methane emissions partially offset "blue carbon" burial in mangroves

Judith A. Rosentreter[1]*, Damien T. Maher[1,2], Dirk V. Erler[1], Rachel H. Murray[1], Bradley D. Eyre[1]

Organic matter burial in mangrove forests results in the removal and long-term storage of atmospheric CO_2, so-called "blue carbon." However, some of this organic matter is metabolized and returned to the atmosphere as CH_4. Because CH_4 has a higher global warming potential than the CO_2 fixed in the organic matter, it can offset the CO_2 removed via carbon burial. We provide the first estimate of the global magnitude of this offset. Our results show that high CH_4 evasion rates have the potential to partially offset blue carbon burial rates in mangrove sediments on average by 20% (sensitivity analysis offset range, 18 to 22%) using the 20-year global warming potential. Hence, mangrove sediment and water CH_4 emissions should be accounted for in future blue carbon assessments.

INTRODUCTION

Climate change, driven primarily by increased atmospheric CO_2 concentrations, is one of the most significant global environmental issues facing the planet (*1*). Mitigation strategies include emission reduction and preserving and enhancing natural carbon stores. Most conservation programs have focused on the restoration of terrestrial ecosystems such as tropical rainforests and enhancing carbon reserves in agricultural farmland (*2*–*4*). More recently, the disproportionally large role of coastal vegetated ecosystems as efficient natural carbon sinks has been highlighted (*5*, *6*). The term "blue carbon" was coined to describe carbon burial in vegetated coastal ecosystems such as mangrove forests, seagrass beds, and salt marshes (*7*–*9*). Although vegetated coastal habitats cover a relatively small area (<2%) of the coastal ocean, they have burial rates 40 times higher than tropical rainforests and account for more than half of the carbon burial in marine sediments (*8*).

Mangrove forests are highly productive ecosystems and one of the most carbon-rich ecosystems in the world (*10*, *11*). The total net primary production (NPP) of mangroves is approximately 200 Tg C $year^{-1}$ (*12*, *13*), but most of this carbon is lost or recycled via CO_2 flux to the atmosphere (34.1 Tg C $year^{-1}$, ~20%) or exported as particulate organic carbon (POC), dissolved organic carbon (DOC), and dissolved inorganic carbon (DIC) to the ocean (117.9 Tg C $year^{-1}$; ~60%) (*13*, *14*). Of the remaining carbon, burial accounts for between 18.4 and 34.4 Tg C $year^{-1}$ (*5*, *11*, *12*, *15*), and this blue carbon is considered a significant long-term storage of atmospheric CO_2 (Fig. 1). Mangrove ecosystems have been promoted as efficient natural carbon sinks (*5*, *7*). However, on a global scale, annual mangrove blue carbon burial represents only about 0.2 to 0.3% of global anthropogenic CO_2 emission [mainly fossil fuel and deforestation, ~10 Pg C $year^{-1}$ (*1*)]. Furthermore, during the process of carbon burial, methanogenic archaea produce CH_4 in anoxic sediments (*16*, *17*). Because CH_4 has a global warming potential (GWP) that is 34 to 86 times more powerful than CO_2 (*1*), CH_4 emissions have the potential to offset a part of the CO_2 initially removed from the atmosphere and buried as blue carbon. However, there is no estimate of the global magnitude of this potential offset.

Mangrove forests are intertidal ecosystems, and although they are net autotrophic on a whole ecosystem scale, sediments and creek waters are generally sources of CO_2 (and CH_4) to the atmosphere. Along the tidal elevation gradient (creek to forest basin), the mangrove type, microbial processes, and sediment structure can change markedly. The intersite variability of mangrove ecosystems is primarily related to geophysical energies as well as climatic and geomorphological conditions such as the relative influence of rainfall, tidal amplitude, exposure to strong water movement, bed rock composition, and the local vegetation and fauna (*18*). Emissions of CH_4 from mangrove sediments are highly variable but are generally larger than emissions from creek waters and can be enhanced in the presence of plant roots and pneumatophores (*19*–*21*). The few published water-to-atmosphere CH_4 flux rates from India, Tanzania, Thailand, and Australia range from 6.3 to 828 μmol m^{-2} day^{-1}, also suggesting high variability of CH_4 emissions from mangrove waters [for example, see the studies of Barnes *et al.* (*22*), Call *et al.* (*23*), and Linto *et al.* (*24*)].

Here, we use new data on seasonal (wet and dry) CH_4 emissions from three mangrove creeks in tropical Australia and previously published water-atmosphere and sediment-atmosphere flux rates to revise estimates of global mangrove CH_4 emissions. We then compare updated CH_4 emissions to revised estimates of global carbon burial rates using published data to calculate the degree to which blue carbon storage in mangrove forests may be offset by CH_4 emissions.

RESULTS

Tidal dynamics and physicochemical parameters

The tidal amplitude was highest in the Fitzroy River (FR) mangrove creek (2.9 to 4.4 m), followed by the Johnstone River (JR) (1.5 to 1.9 m) and the Burdekin River (BR) mangrove creek (1.2 to 1.7 m). Similarly, tidal currents were highest in the FR mangrove creek (pronounced in the wet season) with current velocity ranging from 2.2 to 90.1 cm s^{-1}. In the BR and JR, current velocities were similar, with values between 0.1 and 35.5 cm s^{-1} (table S1). We measured high salinities in the BR (from 27.8 to 36.4). Salinities at the FR and JR mangrove study sites were lower, ranging from 5.5 to 35.7 and 0.4 to 23.4, respectively (table S1). Water temperature ranged between 19° and 29°C during the wet and dry seasons. Wind speed (u) was up to 7.9 m s^{-1} in the FR, 7.7 m s^{-1} in the BR, and generally lower in the JR (0 to 5.9 m s^{-1}; table S1).

CH_4 concentrations and flux rates in the BR, FR, and JR mangrove creeks

We found high temporal and intersite variability of CH_4 concentrations overall, ranging from 6 to 1069 nM in the BR, FR, and JR (Fig. 2).

[1]Centre for Coastal Biogeochemistry, School of Environment, Science and Engineering, Southern Cross University, Lismore, New South Wales 2480, Australia. [2]Southern Cross Geoscience, Southern Cross University, Lismore, New South Wales 2480, Australia.
*Corresponding author. Email: judith.rosentreter@scu.edu.au

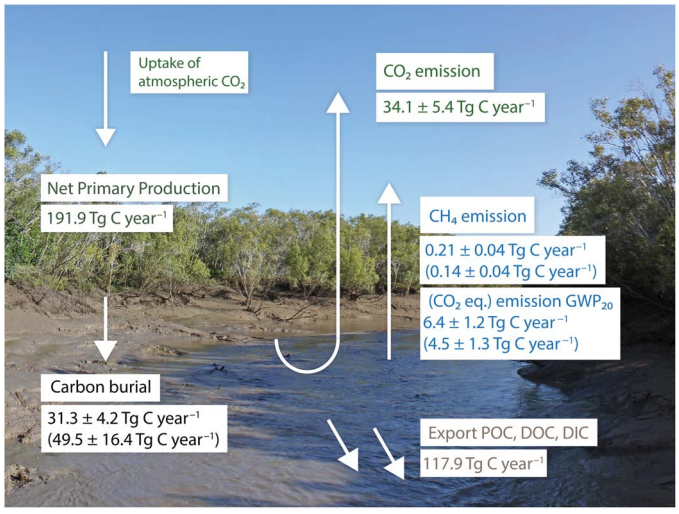

Fig. 1. Mangrove NPP versus mangrove carbon loss. The mangrove NPP of 191.9 Tg C year^{-1} and tidal exports of POC (25.6 Tg C year^{-1}), DOC (13.7 Tg C year^{-1}), and DIC (78.6 Tg C year^{-1}) are derived from Alongi and Mukhopadhyay (*13*) and scaled to the total global mangrove area estimate of Giri *et al.* (*25*). Global mangrove CO_2 emissions of 34.1 ± 5.4 Tg C year^{-1} are from Rosentreter *et al.* (*14*). Global mangrove CH_4 emissions are further presented as CO_2 equivalent emissions using the GWP_{20} (Table 2). The values presented in brackets are the latitudinal scaled total CH_4 emission and burial rates (Table 3). Photo used with permission from A. McMahon.

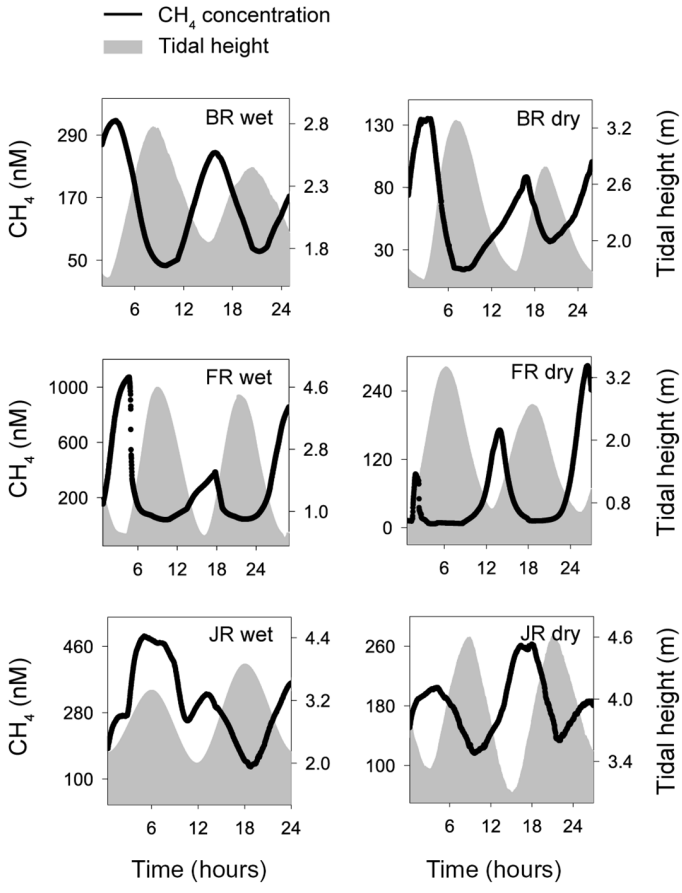

Fig. 2. CH_4 concentrations over two tidal cycles. CH_4 concentration (nM) at the mangrove sites in the BR, FR, and JR estuaries in the wet and dry season.

Concentrations of CH_4 followed a clear tidal pattern, with highest concentrations at low tide and lowest concentrations at high tide. An exception was in the JR in the wet season, where CH_4 concentrations peaked during the first high tide. No general pattern was found between surface water CH_4 concentration and salinity (Fig. 3). In the BR mangrove creek, CH_4 concentrations increased toward higher salinities. In the JR mangrove creek, CH_4 concentrations decreased toward higher salinities, and in the FR, surface water CH_4 and salinity displayed a hysteresis pattern.

Water-to-atmosphere fluxes of CH_4 were tidally influenced with highest flux rates generally at mid to low tide when currents were strongest and gas concentrations in the water were highest. Table 1 shows the variability of the water-atmosphere CH_4 flux rates depending on the different *k* models used (see Materials and Methods). The CH_4 flux rates calculated based on the empirical models of *H16* and *RC01* were generally lower than those based on the *R17* models. In contrast, CH_4 flux rates based on the *B04* parameterization were always higher compared to the flux rates based on the *R17* parameterizations. Because the empirical models of *R17* were constructed for CH_4 gas transfer (k_{600}-CH_4) at the water-atmosphere interface and were also site-specific for the mangrove creeks in this study, the average of the three parameterizations was used to estimate CH_4 flux rates in the BR, FR, and JR. In the JR in the wet season, no current velocity or water depth data were available, and the *RC01 k* model likely underestimated the actual flux rate in our mangrove creeks (Table 1). For this reason, the difference between *RC01* and the average *R17* flux rate was applied to estimate the CH_4 flux in the JR in the wet season. Overall, water-atmosphere CH_4 flux rates in the three studied mangrove creeks ranged from 96.5 to 1049.8 µmol m^{-2} day^{-1} and were 64, 91, and 40% higher in the wet season compared to the dry season in the BR, FR, and JR, respectively.

Upscaled mangrove CH_4 emissions

Sediment-atmosphere flux rates from previously published studies were on average ~30% higher compared to water-atmosphere fluxes from this study and previously published studies (Table 2). Accounting for intertidal mangrove systems being inundated 50% of the time (water-atmosphere flux) and exposed 50% of the time (sediment-atmosphere flux), average mangrove CH_4 emissions were 339.6 ± 106.2 µmol m^{-2} day^{-1}. Global total CH_4 emissions scaled to the most recent mangrove forest area of 137,760 km^2 (*25*) were 0.273 ± 0.053 Tg CH_4 year^{-1}. Using the conversion factor of the GWP for the 20- and 100-year time horizons, the "CO_2 equivalent" CH_4 emissions correspond to 6.41 ± 1.24 Tg C year^{-1} (GWP_{20}) and 2.53 ± 0.49 Tg C year^{-1} (GWP_{100}). With respect to latitude, we found the largest mangrove CH_4 flux at midlatitudes (20° to 25°; Fig. 4A). This was the case for both sediment-atmosphere fluxes and water-atmosphere fluxes (table S4 and fig. S1). Latitudinal scaled total CH_4 emissions were 0.191 ± 0.057 Tg CH_4 year^{-1}, and latitudinal scaled total CO_2 equivalent CH_4 emissions were 4.47 ± 1.34 Tg C year^{-1} and 1.77 ± 0.53 Tg C year^{-1} for the GWP_{20} and GWP_{100}, respectively (Table 3).

Upscaled mangrove burial rates

Published average burial rates ranged from 56.60 to 651.0 g C m^{-2} year^{-1} based on 27 study sites (Table 2 and table S5). Global total burial rates scaled to the total mangrove area of 137,760 km^2 were, on average, 31.30 Tg C year^{-1} (range, 7.80 to 89.68 Tg C year^{-1}). Latitudinal scaled total burial rates were higher than total global burial rates, with

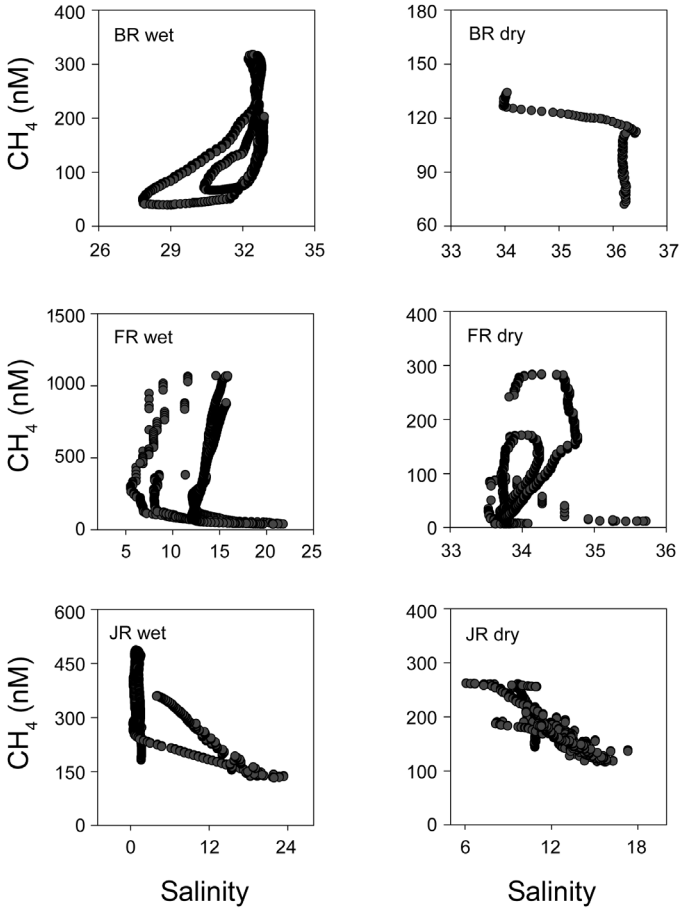

Fig. 3. CH_4 concentrations versus salinity. CH_4 concentration (nM) over the salinity range during the 24-hour time series in the wet and dry season in the BR, FR, and JR mangrove creeks. The salinity in the BR dry season is only available for the first 3 hours of the time series. Note the different scale of salinity in each system.

an average of 49.48 ± 16.4 Tg C $year^{-1}$ (Table 3). Figure 4B shows the average burial rates over the latitudinal regions 0° to 40° in 5° steps. Burial rates showed a weak increase toward the lower latitudes.

Carbon burial offsets by CH_4 emissions

Global total carbon burial offsets by CH_4 emissions (based on the GWP_{20}) were 20.5%, and the sensitivity analysis offsets ranged from 19.8 to 21.0% (Table 2). Global CH_4 emission offsets scaled over the latitudes 0° to 40° were similar, with an average of 20.1% and a sensitivity analysis offset range of 17.7 to 22.0% (Table 3). We found the highest average offset (~65%) at the midlatitudinal region 20° to 25°. The largest unknowns are the average offsets calculated for the latitudinal regions 30° to 40° and 0° to 5° due to the lack of measured CH_4 emission rates (and carbon burial between 30° and 40°). The regions 30° to 35° and 35° to 40° have very small areas of mangroves and therefore have little impact on overall global offsets; however, the 0° to 5° latitudinal region has a large area of mangroves and will influence the overall global offsets.

DISCUSSION

Variability of CH_4 emissions from mangrove ecosystems

We calculated water to atmosphere CH_4 flux rates for the FR, BR, and JR mangrove creeks in two field campaigns in the wet and dry season. The evasion rates (96.5 to 1049.8 μmol m^{-2} day^{-1}) are at the high end or higher than previously published CH_4 flux rates for mangrove ecosystems (table S2) (*22*, *23*). This is most likely because CH_4 flux rates vary greatly depending on *k* in the flux computation. In shallow tidal mangrove ecosystems, *k* is mainly controlled by current generated turbulence, and reliable water-to-atmosphere fluxes should therefore be based on site-specific *k* parameterizations that include current velocity (*26*, *27*). In addition, our study measured in situ CH_4 concentrations continuously (<1 s), and water-atmosphere flux rates were calculated at high resolution (per minute). Most previous studies calculated CH_4 emissions based on discrete sampling that can miss some of the tidally influenced temporal variability that is evident in our data (*20*, *22*, *24*).

Water CH_4 evasion rates were significantly higher (40 to 91%) in the wet season compared to the dry season (Table 1). Higher flux rates in the wet season (>17%) were also found in the mangrove waters of the Andaman Islands (*24*) and may be driven by freshwater riverine inputs that increase nutrient loading, increase the supply of labile organic matter, and reduce the supply of sulfate (and therefore inhibit sulfate reduction), all of which can enhance CH_4 production rates (*19*, *28*).

In the three studied mangrove creeks, surface water salinity was always lower in the rainy season. No clear pattern was observed between surface water CH_4 concentration and salinity (Fig. 3). Surface water salinity covaried with other drivers of CH_4 emissions such as tidal height and pore water flushing. The inverse relationship of surface water CH_4 concentrations and tidal height is indicative of tidal pumping—the exchange of CH_4-enriched (and CO_2-, DIC-, and alkalinity-enriched) groundwater or sediment pore water with surface water (*29*–*31*), which has been found in previous studies driving high surface water CH_4 (Fig. 2) (*22*–*24*). However, in the JR in the wet season, the enhanced CH_4 concentrations during the first high tide were likely driven by freshwater flushing to the mangrove creek (salinity during the first high tide ranged from 0.5 to 1.6; table S1). With regard to this offset exercise, we assumed that sediment-atmosphere and water-atmosphere emissions as well as carbon burial are autochthonous, but further research in this area is needed.

The literature review showed that CH_4 fluxes from exposed mangrove sediments are highly variable (0 to 2127.2 μmol m^{-2} day^{-1}) but generally larger than emissions from the mangrove creek waters (Table 2). This is consistent with the findings of a study in two Tanzanian mangrove forests, where the highest CH_4 emissions occurred at low tide (exposed sediments) and the lowest CH_4 emissions occurred at high tide (inundated) (*20*). During the high tide, increased hydrostatic pressure can inhibit CH_4 emissions (*32*). Furthermore, CH_4, that is, fluxes at the sediment-water interface, can be oxidized by methane-oxidizing bacteria before it reaches the atmosphere (*33*). At low tide, the flux through pneumatophores, plant roots, and crab burrows can further enhance total CH_4 emissions from sediments (*20*, *21*); however, the emitted CH_4 originates from methanogenesis of the surrounding sediments and not from the plant roots or crabs themselves. Ebullition is a major flux component in shallow freshwater ecosystems with high organic matter supply (*34*, *35*) and may also contribute to total CH_4 emissions from mangrove sediments. In the three studied mangrove creeks, there was no ebullition from sediments, and results from 209 floating chamber deployments measuring water-atmosphere CH_4 fluxes did not show any evidence of ebullition (*27*). To our knowledge, only one published study measured CH_4 concentration in sediment gas bubbles (*21*), but we actively stirred the gas bubbles from the Pichavaram mangrove sediments and therefore do not consider them naturally occurring ebullition. Ebullition from sediments and other tree-mediated

Table 1. Average (± confidence interval) water-atmosphere CH_4 flux rates and gas transfer velocities using different empirical *k* models. na, not available.

k model	Variables*	BR wet		BR dry		FR wet		FR dry		JR wet		JR dry	
		flux (µmol m^{-2} day^{-1})	k_{600} (cm $hour^{-1}$)	flux (µmol m^{-2} day^{-1})	k_{600} (cm $hour^{-1}$)	flux (µmol m^{-2} day^{-1})	k_{600} (cm $hour^{-1}$)	flux (µmol m^{-2} day^{-1})	k_{600} (cm $hour^{-1}$)	flux (µmol m^{-2} day^{-1})	k_{600} (cm $hour^{-1}$)	flux (µmol m^{-2} day^{-1})	k_{600} (cm $hour^{-1}$)
R17 (*27*)	*v*	236.5 ± 7.4	5.7	103.7 ± 3.6	7.3	1059.0 ± 48.9	15.0	95.3 ± 6.4	8.3	na	na	484.4 ± 9.4	9.8
R17 (*27*)	*v*, *u*	283.7 ± 8.3	6.8	104.6 ± 4.3	6.9	1110.7 ± 49.5	16.4	99.2 ± 6.8	8.9	na	na	460.4 ± 9.6	9.3
R17 (*27*)	*v*, *u*, *h*	324.7 ± 8.8	7.9	115.7 ± 4.3	7.7	979.8 ± 40.7	15.5	94.8 ± 6.3	9.0	na	na	535.3 ± 8.7	10.9
Average flux (*R17*)		301.0 ± 8.7	6.8	108.0 ± 4.0	7.3	1049.8 ± 46.3	15.6	96.5 ± 6.5	8.7	826.2†	10.2†	493.3 ± 9.1	10.0
H16 (*26*)	*v*, *u*, *h*	275.0 ± 9.8	6.5	69.1 ± 3.6	3.8	601.4 ± 28.3	8.1	69.6 ± 4.9	6.0	na	na	167.0 ± 4.5	3.4
RC01 (*54*)	*u*	385.0 ± 13.8	9.2	93.5 ± 4.9	5.0	474.7 ± 17.1	8.1	74.8 ± 5.1	7.1	375.2 ± 8.7	4.7	224.0 ± 5.8	4.6
B04 (*55*)	*v*, *u*, *h*	623.2 ± 18.0	14.7	187.4 ± 7.8	10.9	1542.7 ± 75.7	19.3	191 ± 13.2	15.6	na	na	494.7 ± 10.1	10.2

*Current velocity (*v*) in cm s^{-1}, water depth (*h*) in m, and wind speed (*u*) in m s^{-1}. †Calculated based on the % difference of *RC01* and average *R17* in the JR dry season.

Table 2. Global CH_4 emissions, carbon burial rates, and offsets in mangroves. Global emission and carbon burial rates are upscaled to the global mangrove forest area of 137,760 km^2 (*25*). *n* refers to the number of study site locations (see tables S2, S3, and S5).

	CH_4 flux rate (µmol m^{-2} day^{-1})	Global CH_4 emission (Tg CH_4 $year^{-1}$)	Global CH_4 emission (Tg C $year^{-1}$)	CH_4 (CO_2 eq.) emission, GWP_{20} (Tg C $year^{-1}$)	CH_4 (CO_2 eq.) emission, GWP_{100} (Tg C $year^{-1}$)	Sequestration rate (g C m^{-2} $year^{-1}$)	Global carbon burial (Tg C $year^{-1}$)	Offset (%)*	Sensitivity analysis offset range (%)†
Water-air CH_4 flux	(*n* = 9)	(*n* = 9)	(*n* = 9)	(*n* = 9)	(*n* = 9)	(*n* = 27)	(*n* = 27)		
Min	35.10	0.028	0.021	0.66	0.26	56.60	7.80		
Max	659.8	0.531	0.398	12.45	4.92	651.0	89.68		
Average ± SE	288.0 ± 73.2	0.232 ± 0.059	0.174 ± 0.044	5.43 ± 1.38	2.15 ± 0.55	227.2 ± 30.67	31.30 ± 4.22	17.3	(15.7–18.5)
Sediment-air CH_4 flux	(*n* = 14)	(*n* = 14)	(*n* = 14)	(*n* = 14)	(*n* = 14)	(*n* = 27)	(*n* = 27)		
Min	0	0	0	0	0	56.60	7.80		
Max	2,127.2	1.71	1.28	40.14	15.87	651.0	89.68		
Average ± SE	391.2 ± 153.4	0.315 ± 0.123	0.236 ± 0.093	7.38 ± 2.90	2.92 ± 1.14	227.2 ± 30.67	31.30 ± 4.22	23.6	(22.0–25.8)
Global total	(*n* = 23)	(*n* = 23)	(*n* = 23)	(*n* = 23)	(*n* = 23)	(*n* = 27)	(*n* = 27)		
Average ± scaled error	339.6 ± 106.2‡	0.273 ± 0.053‡	0.205 ± 0.040‡	6.41 ± 1.24‡	2.53 ± 0.49‡	227.2 ± 30.67	31.30 ± 4.22	20.5	(19.8–21.0)

*Offset is calculated from carbon burial (Tg C $year^{-1}$) and the CH_4 flux using the GWP_{20} (Tg C $year^{-1}$). †Carbon burial (Tg C $year^{-1}$) and CH_4 emissions (GWP_{20}; Tg C $year^{-1}$) are adjusted up and down by their errors. ‡Accounting for mangrove ecosystems being inundated 50% of the time (water-atmosphere flux) and exposed 50% of the time (sediment-atmosphere flux).

(stems and leaves) CH_4 emissions is not sufficiently available for mangrove ecosystems and hence we could not incorporate it in our mangrove CH_4 emission estimate. Our global CH_4 emission and corresponding carbon burial offsets may therefore be underestimated and should be seen as a lower-bound estimate.

Latitudinal mangrove carbon burial rates increased toward lower latitudes (Fig. 4B), which is consistent with an early review of carbon burial in mangrove sediments over four latitudinal zones (*18*). The average carbon sequestration rate proposed by Twilley *et al.* (*18*) is, however, much lower (100 g C m^{-2} $year^{-1}$) than the latitudinal average estimate in this study (269.2 ± 73.7 g C m^{-2} $year^{-1}$). There is also a similar latitudinal trend for mangrove aboveground and belowground biomass (*18*, *36*), mangrove litter fall (*37*), and soil carbon stocks (*18*, *36*). Mangrove production (NPP) is also higher at the tropical west Pacific region between the Sunda Sea and Philippine Sea (approximately 0° to 10°) compared to higher latitudinal regions such as the west Indian coast of Africa or the northeast Pacific region between Mexico and Panama (*13*). Average CH_4 emissions were highest in mangroves at midlatitudes. However, there is a lack of CH_4 emission data from sediments and the water column at low latitudes (<10°; Fig. 5 and fig. S1). Generally higher temperatures and precipitation in tropical/monsoonal climate zones suggest that mangroves of the wet tropics may be more productive and have higher carbon burial rates and CH_4 emissions than mangroves of the dry tropics (*13*). Ouyang *et al.* (*38*) also found that the impact of geographic (latitude), climatic, and biotic (ecosystem type) drivers influences mangrove root decomposition rates. In particular, mangrove type (for example, riverine, fringe, and overwash) and mangrove species have a strong influence on the rates of mangrove root decomposition and root decay rates (*38*). There was no obvious pattern between mangrove species, mangrove type, and CH_4 emissions. Certainly, more data on CH_4 emissions and carbon burial rates from different geographic and climatic regions, different mangrove ecosystem types, and levels of disturbance would help to better explore these relationships.

Latitudinal scaled total CH_4 emissions were 30% lower than CH_4 emissions that were upscaled to the total mangrove forest area (Tables 2 and 3). Latitudinal scaled burial rates were 37% higher than global scaled burial rates. The discrepancy may be explained by the few data that are available for latitudes 0° to 10° and >30°. We estimated the missing CH_4 emissions and burial rates of these latitudinal regions from the next closest latitudinal region or are the average of the next two closest regions (Fig. 4 and table S4). Hence, the accuracy of the CH_4 emission and carbon burial estimates for these regions is unknown. Because we also used the low water CH_4 flux for 5° to 10° for the latitudinal region 0° to 5° and did not observe any sediment CH_4 emissions for 0° to 5° latitudes (table S4), we applied a low average CH_4 flux rate (40.3 µmol m^{-2} day^{-1}) to 54% of the total mangrove area, resulting in lower latitudinal scaled CH_4 emissions compared to global total scaled emissions (Fig. 4A and Tables 2 and 3). Similarly, we applied the very high carbon burial rates for the latitudinal region 5° to 10° to 22% of the total mangrove area, resulting in higher latitudinal scaled total carbon burial compared to global total scaled burial (Fig. 4B and Tables 2 and 3). Nevertheless, latitudinal scaled total estimates and the comparison of mangrove emissions and burial over different climatic and latitudinal regions give important insights into global trends and help to reveal hot spots of mangrove CH_4 emissions, carbon burial rates, and hence burial offsets by CH_4 emissions, and highlight areas where further work is required.

The global total and the latitudinal scaled total CH_4 emissions from mangrove ecosystems in this study (0.2 to 0.3 Tg CH_4 $year^{-1}$) are lower than previous estimates (*11*, *22*). The global estimate of 2.2 Tg CH_4 $year^{-1}$ proposed by Barnes *et al.* (*22*) is based on only one study of relatively high CH_4 flux rates in a pristine mangrove creek on the Andaman Islands (552 to 828 µmol m^{-2} day^{-1}) and upscaled to a

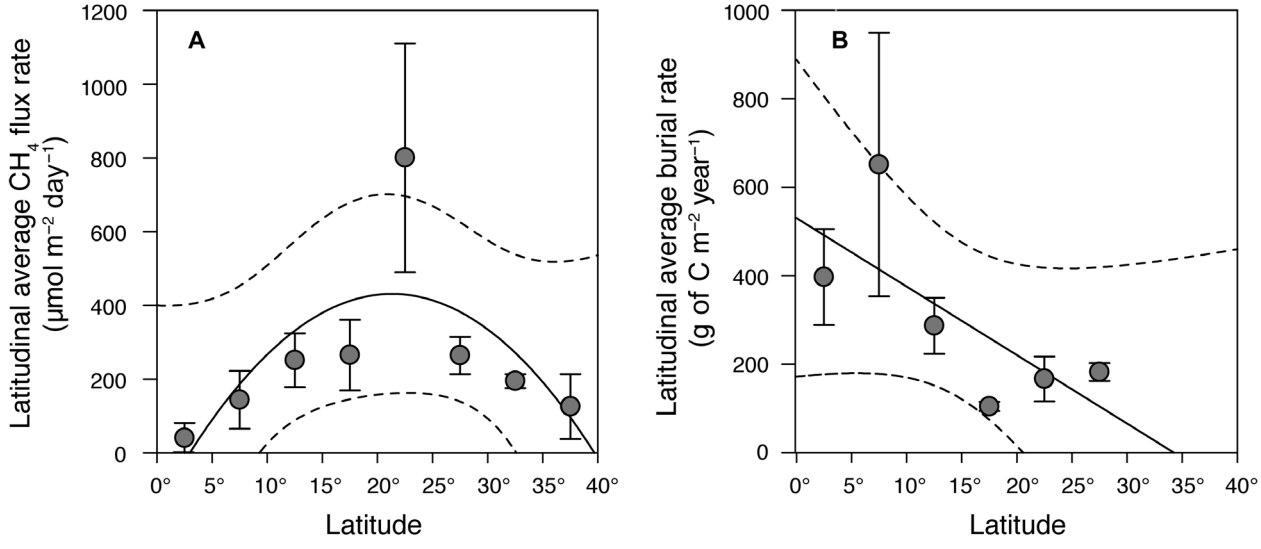

Fig. 4. Latitudinal average mangrove CH_4 flux rates and carbon burial rates. (**A**) Combined average sediment-atmosphere and water-atmosphere CH_4 flux rate (±SE) of the latitudinal regions 0° to 40° (in 5° steps), including this study and previously published studies. Note that in latitudinal regions where no water-atmosphere or sediment-atmosphere CH_4 flux data were available, we used the next closest latitudinal region or the average of the next higher and lower latitudinal region (see Materials and Methods and table S4). The black line indicates the quadratic regression line (r^2 = 0.49, n = 8, P < 0.5). (**B**) Average carbon burial rate (±SE) of the latitudinal regions 0° to 30° (in 5° steps) of previously published studies. The black line indicates the linear regression line (r^2 = 0.69, n = 6, P < 0.05). The dashed lines indicate the 95% confidence interval.

Table 3. Latitudinal CH_4 emissions, carbon burial, and offsets in mangroves. Mangrove latitudinal areas are based on Giri *et al.* (*25*). Error (±) is scaled error (see text) unless marked with "[a]" (in these cases, the SE is used).

Latitude	Mangrove area (km^2)	Average CH_4 flux rate ($\mu mol\ m^{-2}\ day^{-1}$)*	Latitudinal CH_4 emission (Tg CH_4 $year^{-1}$)	Latitudinal CH_4 emission (Tg C $year^{-1}$)	Latitudinal CH_4 (CO_2 eq.) emission, GWP_{20} (Tg C $year^{-1}$)	Latitudinal CH_4 (CO_2 eq.) emission, GWP_{100} (Tg C $year^{-1}$)	Average burial rate (g C m^{-2} $year^{-1}$)	Latitudinal carbon burial (Tg C $year^{-1}$)	Offset (%)†	Sensitivity analysis offset range (%)‡
0–5°	44,000	40.26 (± 40.3)[a]	0.010 (± 0.005)	0.008 (± 0.004)	0.24 (± 0.12)	0.10 (± 0.05)	396.6 (± 108.5)[a]	17.45 (± 4.78)	1.4	(1.0–1.6)
5–10°	30,000	143.8 (± 78.3)[a]	0.025 (± 0.013)	0.019 (± 0.009)	0.59 (± 0.29)	0.23 (± 0.12)	651.0 (± 298.0)[a]	19.53 (± 8.94)	3.0	(2.8–3.1)
10–15°	23,500	251.0 (± 72.8)[a]	0.034 (± 0.006)	0.026 (± 0.004)	0.81 (± 0.14)	0.32 (± 0.05)	286.8 (± 63.3)[a]	6.74 (± 1.49)	12.0	(11.5–12.7)
15–20°	16,500	265.1 (± 95.5)[a]	0.026 (± 0.001)	0.019 (± 0.001)	0.60 (± 0.03)	0.24 (± 0.01)	104.4 (± 10.4)[a]	1.72 (± 0.17)	34.8	(33.4–36.5)
20–25°	18,800	800.5 (± 310.4)[a]	0.088 (± 0.032)	0.066 (± 0.024)	2.06 (± 0.75)	0.81 (± 0.30)	166.6 (± 50.7)[a]	3.13 (± 0.95)	65.8	(63.2–67.2)
25–30°	4,300	264.1 (± 50.3)[a]	0.007 (± 0.003)	0.005 (± 0.002)	0.16 (± 0.06)	0.06 (± 0.02)	182.8 (± 19.7)[a]	0.79 (± 0.08)	19.8	(13.5–24.8)
30–35°	310	194.9 (± 18.9)[a]	0.0004 (± 0.0001)	0.0003 (± 0.0001)	0.008 (± 0.003)	0.003 (± 0.001)	182.8 (± 19.7)[a]	0.057 (± 0.006)	14.6	(10.0–18.3)
35–40°	350	125.7 (± 88.1)[a]	0.0003 (± 0.0001)	0.0002 (± 0.0001)	0.006 (± 0.002)	0.002 (± 0.001)	182.8 (± 19.7)[a]	0.064 (± 0.007)	9.4	(6.4–11.8)
	Total	*Average*	*Total*	*Total*	*Total*	*Total*	*Average*	*Total*	*Average*	*Range*
Latitudinal total	137,760	260.6 (± 94.3)[a]	0.191 (± 0.057)	0.143 (± 0.043)	4.47 (± 1.34)	1.77 (± 0.53)	269.2 (± 73.7)[a]	49.48 (± 16.4)	20.1	(17.7–22.0)

*Combined sediment-atmosphere and water-atmosphere flux accounting for mangrove ecosystems being inundated 50% of the time (water-atmosphere flux) and exposed 50% of the time (sediment-atmosphere flux; see table S4). †Offset is calculated from carbon burial (Tg C $year^{-1}$) and the CH_4 flux using the GWP_{20} (Tg C $year^{-1}$). ‡Carbon burial rates (Tg C $year^{-1}$) and CH_4 emissions (GWP_{20}, Tg C $year^{-1}$) are adjusted up and down by their scaled errors.

mangrove area of 360,000 km^2. A more recent global estimate is even higher (5 Tg C $year^{-1}$) (*11*). This estimate used the same mangrove area estimate that we used in this study (*25*), but it was unclear what data were included in their estimate and how they were calculated. Although there are still relatively high uncertainties in the upscaled mangrove CH_4 emissions presented in this study, our global estimates include previously published sediment and water CH_4 emissions, newly measured seasonal data of CH_4 fluxes from three mangrove ecosystems, and upscaling by latitudinal region, which is an important control of CH_4 emissions.

Mangrove CH_4 emissions partially offset mangrove carbon burial

Global total and latitudinal scaled carbon burial offsets by CH_4 emissions are similar and estimated to be ~20% (Tables 2 and 3). The global total mangrove carbon burial estimate in this study (31.3 ± 5.2 Tg C $year^{-1}$) is in agreement with previous mangrove carbon burial estimates (18.4 to 34.4 Tg C $year^{-1}$) (*5*, *11*, *12*, *15*) and accounts for approximately 16% of mangrove NPP (Fig. 1). We expected this because all the previous estimates were also based on upscaling average carbon burial rates to the global total mangrove forest area. In contrast, our latitudinal scaled total burial estimate is higher because it emphasizes denser mangrove forests (biomass) and concomitant higher burial rates at low latitudes [for example, Tamandaré, Brazil, 8.7°S, 651 g C m^{-2} $year^{-1}$ (*39*)]. The lack of carbon burial rates at the latitudinal regions 30° to 35° and 35° to 40° likely underestimates the potential offsets in these regions, but because of the small area of mangroves in these regions, they have little impact on the overall global offset estimates (Table 3). The adjusted offsets are highest at the latitudes 20° to 25°, driven by lower burial rates and high CH_4 emissions. Mangrove biomass and carbon burial decrease toward higher latitudes (*25*, *38*), but emissions of CH_4 may still be high relative to burial rates due to, for example, groundwater inputs and tidal pumping, which can enhance surface water CH_4 (*40*, *41*) but may have a less pronounced effect on burial rates. Carbon burial offsets by CH_4 emissions should therefore be highest at midlatitudes, where burial rates were ~200 g C m^{-2} $year^{-1}$ and CH_4 emissions were ~800 μmol m^{-2} day^{-1} (Table 3).

Measurements of carbon burial rates, sediment, and water CH_4 emissions are available for the same mangrove system in southern Moreton Bay (Australia) (*23*, *42*). Local offsets of carbon burial by CH_4 emissions in southern Moreton Bay were on average 24.1% (range, 19.5 to 28.7%). This is similar to our average global estimates, giving some confidence in the upscaled mangrove CH_4 emissions and carbon burial rates. Although our estimates presented here have relatively large uncertainties (Tables 2 and 3), mangrove CH_4 emissions and offsets

should be accounted for in future mangrove blue carbon assessments and global CH_4 budgets.

Uncertainties of global emissions and future research

The sensitivity analysis and the comparison of offsets over different latitudinal regions (Table 3) show that although there could be a large range in the possible mangrove carbon burial offset by CH_4 emissions, the overall conclusion that there is some offset remains the same. However, there are also several other factors that contribute to the uncertainties in our global CH_4 emission and carbon burial estimates (Tables 2 and 3) that are not accounted for in our error and sensitivity analysis, some of which also influence our partial offsets of carbon burial rates. First, few or no CH_4 flux rates are available for the latitudes 0° to 10° and 30° to 40° (Fig. 5). However, the world's largest mangrove areas are in low latitudinal regions, such as Indonesia (22.6% of global total), Australia (7.1%), or Brazil (7.0%) (*25*). The world's best developed mangrove forests can be found in the Sundarbans, the Mekong Delta, the Amazon, Madagascar, and Southeast Asia (*25*). Further, Indonesia has the highest mangrove species diversity [48 species (*42*)] and exceptionally high carbon stocks in mangrove sediments (*43*). Given the high variability and uncertainties in global mangrove CH_4 emissions, more studies are needed, especially in extensive mangrove forest regions such as the Niger Delta, the West Africa mangrove coast (Rivières du Sud), Indonesia, northern Brazil, and southern Papua.

Second, global mangrove CH_4 emission and carbon burial estimates depend on accurate global mangrove area estimates. Although the global mangrove area proposed by Giri *et al.* (*25*) seems to be the most precise estimate to date (*44*), the Global Land Survey (GLS) data, based on high-resolution 30-m Landsat satellite imagery from U.S. Geological Survey (USGS), cover a period from 1997 to 2000 and do not account for small patches (<2700 m^2), which can make a substantial difference to the total area (*25*). Moreover, the loss of mangrove forest due to natural and anthropogenic impacts is occurring globally (*43*, *45*, *46*). Loss rates vary greatly between countries, ranging from 1 to 20% of the total mangrove forest area, which makes it difficult to predict global mangrove forest changes in the future (*47*). Duke *et al.* (*48*) predict a mangrove loss rate of 1 to 3% per year. The decline of mangroves is largely attributed to anthropogenic perturbations and disturbance such as mechanical destruction (mariculture/aquaculture ponds), urbanization, land use change, chemical spill, and climate change impacts (*25*, *46*, *48*, *49*). Climate change—particularly sea level rise—may be the biggest threat to mangroves in future decades (*46*, *50*). An update of global and latitudinal mangrove area estimates would help to better constrain global mangrove CH_4 emissions and their implication on global CH_4 budgets. Although the area estimates influence the amount of carbon buried and the amount of CH_4 emitted by mangroves globally, they do not affect the offset estimates because both terms use the same area.

Data collection and sampling strategy may also be responsible for some variation of global CH_4 flux estimates. Most of the previous published CH_4 flux rates are based on discrete sampling. To account for tidal variability, high-resolution (1 min) continuous sampling of CH_4 concentrations and ancillary data in mangrove waters allows more accurate estimates of CH_4 emissions. For annual estimates, seasonal measurements will be required. Furthermore, our CH_4 emission estimate does not account for potential ebullition from sediments or tree-mediated (stems and leaves) fluxes. More studies are needed not only on different CH_4 emission pathways in mangrove ecosystems but also on mangrove NPP production rates (for example, belowground wood production).

Finally, we want to emphasize that we attribute uncertainties and the variability of CH_4 flux rates, to a certain extent, to the uncertainty of the gas transfer velocity in the flux computation. k_{600}-CH_4 in our three mangrove creeks was on average 9.7 ± 0.9 cm $hour^{-1}$ (range, 5.7 to 16.4 cm $hour^{-1}$; Table 1), hence slightly higher than the average k_{600}-CO_2 that we estimated for the same mangrove sites (7.5 ± 1.1 cm $hour^{-1}$) in a previous study (*14*). In tidal mangrove ecosystems, CH_4 flux rates may be most accurate when based on kCH_4 parameterizations that include current velocity, water depth, and wind speed (*26*, *27*) and account for a nondiffusive microbubble flux component in addition to the diffusive flux of CH_4 across the water-atmosphere interface [for example, see the studies of Rosentreter *et al.* (*27*), McGinnis *et al.* (*51*), and Prairie and del Giorgio (*52*)]. However, there is still a need to further explore the behavior and the drivers of gas transfer velocities of greenhouse

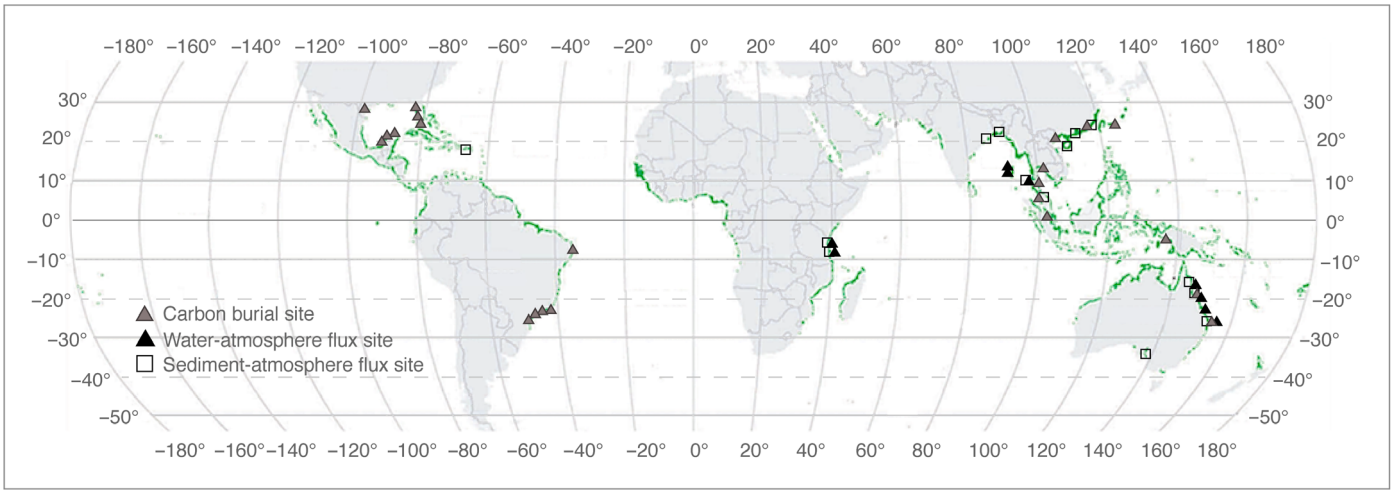

Fig. 5. Map of CH_4 emission studies and carbon burial studies in mangroves. Gray triangles are mangrove carbon burial study sites (table S5). Black triangles are mangrove water-atmosphere CH_4 flux study sites (table S2). Open squares are mangrove sediment-atmosphere CH_4 flux study sites (table S3). Mangrove forest distribution is in green. Map based on the global mangrove forest distribution of Giri *et al.* (*25*).

gases (CO_2, CH_4, and N_2O) at the aqueous boundary layer, particularly in tidally influenced systems such as mangrove ecosystems.

CONCLUSION

The preservation and enhancement of natural carbon stores are part of global climate change mitigation strategies. Despite offering valuable ecosystem services to the coastal zone and its inhabitants, coastal vegetated ecosystems also stand out as large natural carbon stores. The term "blue carbon" was coined to describe the carbon captured in coastal habitats such as mangrove forests, seagrass beds, and salt marshes. Mangrove forests, in particular, are highly productive ecosystems with global carbon sequestration rates that are disproportionate to their area. However, here, we show that CH_4 emissions from mangrove waters have the potential to offset blue carbon burial rates in sediments on average by 20% (sensitivity analysis offset range, 18 to 22%). Hence, CH_4 emissions from mangroves need to be accounted for when assessing their importance in climate change mitigation.

MATERIALS AND METHODS

Study locations

This study compares three mangrove creek sites in different estuaries in the wet and dry seasons, located in the tropical convergence zone along the north-eastern coast of Queensland, Australia. The mangrove-dominated FR estuary (23°31′22.8″S, 150°52′30.0″E), the BR estuary (19°41′13.2″S, 147°36′39.6″E), and the JR estuary (17°30′32.4″S, 146°3′47.6″E) all discharge into the Great Barrier Reef lagoon. In general, the estuaries are dominated by episodic, short-lived, large freshwater inputs during the wet season and low or no discharge and high evaporation rates during the dry season. The river catchments are characterized by different degrees of anthropogenic impacts. Disturbance is higher (mainly land use change) in the JR catchment compared to the FR and BR catchments. Mangroves, predominantly *Avicennia*, *Rhizophora*, and *Ceriops*, cover a large area of the coast and fringe of the estuaries with an overall area of 178 km^2.

Experimental design

Time series of 24 hours were conducted in February/March 2014 (wet season) and September/October 2014 (dry season) in small mangrove creeks in the FR, BR, and JR estuaries. CH_4 concentrations were measured using a cavity ring-down spectroscopy analyzer (G2201-*i*; Picarro). Briefly, water was pumped from a depth of ~30 cm by a submersible pump to a shower-head exchanger, where water was sprayed into a chamber, creating fine droplets that maximize gas equilibration. From the equilibrator, a continuous air loop was linked to the Picarro analyzer, where CH_4 was measured (±60 parts per billion) in the dried gas stream (Drierite desiccant, water vapor maintained at <0.1%) before returning back to the equilibrator. Creek water was pumped into a flow-through chamber on board, where ancillary data (salinity, temperature) were measured every 5 min using a calibrated HydroLab logger (DS5X Sonde, AquaLab). Water current velocity, depth, and direction were detected every 10 min using an acoustic Doppler current profiler (Argonaut-XR-Flowmeter, SonTek), which was deployed at the water bottom a minimum of 5 m away from the boat to ensure no interference with boat movements. A weather station (150 WX, Airmar) was attached on top of the boat to measure wind speed and wind direction every minute over the 24-hour time series.

Flux computation

Water to atmosphere CH_4 fluxes were calculated using the equation

$$F = k\,K_0(C_w - C_a) \quad (1)$$

where F is the flux of CH_4 across the water-atmosphere interface, k is the gas transfer velocity (m day^{-1}), K_0 is the solubility coefficient depending on temperature and salinity, C_w is the partial pressure of CH_4 in the water, and C_a is the partial pressure of CH_4 in the atmosphere. For the flux computation, we used a range of k values derived from different empirical models. First, a recent study determined k models for the same mangrove systems (BR, FR, and JR) using an improved design of the floating chamber method (*R17*) (*27*). The first parametrization accounts solely for current velocity (v)

$$k_{600} - CH_4 = 2.03 + 0.43v \quad (2)$$

where k_{600} (cm $hour^{-1}$) is the gas transfer velocity normalized to the Schmidt number of 600 as a function of temperature and salinity (*53*). The second parameterization accounts for v and wind speed calculated to the height of 10 m over water surface (u)

$$k_{600} - CH_4 = -0.77 + 0.45v + 0.92u \quad (3)$$

The third parameterization accounts for v, u, and water depth (h)

$$k_{600} - CH_4 = -1.07 + 0.36v + 0.99u + 0.87h \quad (4)$$

CH_4 flux rates were further compared to the k_{600} parameterization suggested by Ho *et al.* (*26*) (*H16*), which was determined from a dual tracer ($^3He/SF_6$) release experiment in a mangrove estuary in the Everglades National Park in Florida, also accounting for current velocity, wind speed, and water depth. The wind speed parameterization of Raymond and Cole (*54*) (*RC01*) was suitable for CH_4 flux calculation in the JR wet season, where only wind speed data were available. Finally, CH_4 flux rates were calculated using the parameterization of Borges *et al.* (*55*) (*B04*), which was constructed for estuarine environments.

Global mangrove area estimates

Mangrove area estimates before 2007 ranged from 110,000 to 240,000 km^2 (Food and Agriculture Organization, 2003). The area range has decreased to 152,361 and 137,760 km^2 due to recent availability of high-resolution imagery (*25*, *49*). The mangrove area estimate of 137,760 km^2 by Giri *et al.* (*25*) was generated from GLS data from 1997 to 2000 by Landsat 30-m-resolution satellite imagery provided by the USGS (*25*) and is currently the most precise mangrove forest area estimate (*44*).

Global mangrove CH_4 emissions

The percent inundated and exposed area in the BR, FR, and JR mangrove creeks was estimated based on digital elevation model data (1-m grid interval; precision, ±0.15 m) derived from airborne laser scanning surveys (LiDAR, Department of Natural Resources and Mines, State of Queensland, 2013). The BR mangrove sediments were exposed 52% of the time over the two tidal cycles. The FR mangrove sediments were exposed 42%, and the JR mangrove sediments were exposed 88% of the time. Average CH_4 emissions from this study and previously published studies were calculated, accounting for tidal mangrove systems

being inundated 50% of the time (water-atmosphere flux) and exposed 50% of the time (sediment-atmosphere flux). Water-atmosphere CH_4 flux rates (μmol m^{-2} day^{-2}) are based on different empirical k models in our study and previously published studies. Only studies that were conducted in tidal mangrove creeks were included in global flux estimates. Studies from outer estuaries and open lagoons adjacent to mangroves were excluded because they may be more indicative of marine than mangrove environments. Sediment-atmosphere fluxes that were included were measured using static chamber studies over (low tide) bare sediments and also include plant-mediated flux (pneumatophores and roots), crab burrows, and different tidal zones. Only Scopus-listed publications were included, because some studies published in non–Scopus-listed journals that meet the above criteria did not adequately describe their methodology and calculations or present their data, and therefore, it was uncertain whether the data were reliable.

Two different approaches were used to upscale CH_4 flux rates to global mangrove CH_4 emissions. First, the average CH_4 flux rate is scaled to the total global mangrove forest area of 137,760 km^2 (the "global total") (*25*). Second, we estimate latitudinal average CH_4 flux rates over the latitudes 0° to 40° in 5° steps. At latitudinal regions where no CH_4 flux data (water-atmosphere or sediment-atmosphere) were available, the next closest latitudinal region or the average of the next higher and lower latitudinal region was used (table S4). The average CH_4 flux rate of each latitudinal region was then scaled to the mangrove forest area estimate at each latitudinal region (*25*) and summed up to a global total estimate (the "latitudinal total"). Global total and latitudinal scaled total mangrove CH_4 emissions are presented in Tg CH_4 $year^{-1}$ and Tg C $year^{-1}$.

CH_4 "equivalent CO_2" emissions

We account for CH_4 emissions as CO_2 equivalent emissions using the GWP. The most recent GWPs of CH_4 are 86 and 34 for the time horizons 20 and 100 years, respectively, including climate-carbon feedbacks (*1*). The choice of time horizon has a strong effect on the GWP values and hence the calculated CO_2 equivalent emissions. In the case of CH_4, the GWP decreases by approximately a factor of 3 for a changing time horizon from 20 to 100. The time horizon usually used for GWPs is 100 years; however, the 20-year GWP prioritizes gases with shorter lifetimes such as CH_4 [lifetime, 9.1 ± 0.9 years (*56*)]. Nevertheless, for the best comparison, we present CO_2 equivalent emissions of CH_4 for the GWP_{20} and GWP_{100} time horizons

$$CH_4(CO_2eq.)\ \text{emission} = CH_{4emission} \times GWP \times f \quad (5)$$

where $CH_{4emission}$ is the mangrove CH_4 emission expressed in Tg CH_4 $year^{-1}$; GWP is 86 and 34 for the time horizons 20 and 100, respectively; and f is the conversion factor to Tg C $year^{-1}$ (multiplied by 12/44).

Global carbon burial estimate

The global total and latitudinal total mangrove carbon burial rates were estimated using the same two approaches that were used to estimate global total and latitudinal total mangrove CH_4 emissions. The global total carbon burial is based on published (Scopus-listed) burial sequestration rates in mangrove sediments and upscaled to the total mangrove forest area (*25*). The latitudinal scaled total carbon burial rate is estimated using the average burial rate of each latitudinal region 0° to 40° in 5° steps. Missing burial rates at the latitudinal region 30° to 40° were estimated from the latitudinal region 25° to 30°, upscaled to the mangrove forest area of each latitudinal region (*25*), and summed to a global total estimate.

Global offset calculations

Although the measured CH_4 emissions and carbon burial rates operate over very different timescales, we assumed that CH_4 production has been in steady state over the longer time frame of carbon burial. The global total CH_4 emission offset to global total carbon burial was calculated using the global total CH_4 emission rate (GWP_{20}) and global total carbon burial rate. The latitudinal CH_4 emission offset to latitudinal carbon burial was calculated using the latitudinal CH_4 emission rate (GWP_{20}) 0° to 40° in 5° steps and the corresponding latitudinal carbon burial rate 0° to 40° in 5° steps and averaged over the latitudes 0° to 40°.

Error and sensitivity analysis

Errors for the upscaled estimates were propagated for each carbon burial and CH_4 flux term (F_R)

$$\text{Scaled error} = F_R F_{\%}/100 \quad (6)$$

The % error of each term ($F_{\%}$) was determined [modified from Eyre (*57*)] as

$$F_{\%} = \left((E_R)^2 + (E_M)^2 + (E_R \times E_M)\right)^{0.5} \quad (7)$$

where E_R is the SE of the carbon burial or CH_4 flux rate. The error associated with mangrove area (E_M) was estimated to be ±5% (*57*).

A sensitivity analysis was done, where each of the terms in the global total and latitudinal total offsets were adjusted up and down by their estimated errors to determine if the overall conclusions derived from the upscaling changed [modified from Eyre *et al.* (*58*)]. The CH_4 emissions adjusted down were compared to the carbon burial rates adjusted down, and the CH_4 emissions adjusted up were compared to the carbon burial rates adjusted up. This is because it would be unlikely to get maximum burial rates with minimum CH_4 emissions or minimum burial rates with maximum CH_4 emissions.

SUPPLEMENTARY MATERIALS

Supplementary material for this article is available at http://advances.sciencemag.org/cgi/content/full/4/6/eaao4985/DC1

table S1. Wet and dry season physicochemical parameters and CH_4 concentration in the three studied mangrove creeks.
table S2. Mangrove water-atmosphere CH_4 fluxes from this study and published studies.
table S3. Published mangrove sediment-atmosphere CH_4 fluxes.
table S4. Combined mangrove sediment-atmosphere and water-atmosphere CH_4 fluxes for each latitude region (5° steps).
table S5. Published mangrove carbon burial rates.
fig. S1. Average mangrove CH_4 flux rates over latitudes (5° steps).
References (*59*–*91*)

REFERENCES AND NOTES

1. T. F. Stocker, D. Qin, G.-K. Plattner, M. Tignor, S. K. Allen, J. Boschung, A. Nauels, Y. Xia, V. Bex, P. M. Midgley, *IPCC, 2013: Climate Change 2013: The Physical Science Basis Contribution of Working Group I to the Fifth Assessment Report of the Internovernmental Panel on Climate Change* (Cambridge Univ. Press, 2013).
2. Y. Pan, R. A. Birdsey, J. Fang, R. Houghton, P. E. Kauppi, W. A. Kurz, O. L. Phillips, A. Shvidenko, S. L. Lewis, J. G. Canadell, P. Ciais, R. B. Jackson, S. W. Pacala, A. D. McGuire, S. Piao, A. Rautiainen, S. Sitch, D. Hayes, A large and persistent carbon sink in the world's forests. *Science* **333**, 988–993 (2011).

3. A. Agrawal, D. Nepstad, A. Chhatre, Reducing emissions from deforestation and forest degradation. *Annu. Rev. Environ. Resour.* **36**, 373–396 (2011).
4. P. Smith, D. Martino, Z. Cai, D. Gwary, H. Janzen, P. Kumar, B. McCarl, S. Ogle, F. O'Mara, C. Rice, B. Scholes, O. Sirotenko, M. Howden, T. McAllister, G. Pan, V. Romanenkov, U. Schneider, S. Towprayoon, M. Wattenbach, J. Smith, Greenhouse gas mitigation in agriculture. *Philos. Trans. R. Soc. Lond. Biol. Sci.* **363**, 789–813 (2008).
5. E. Mcleod, G. L. Chmura, S. Bouillon, R. Salm, M. Björk, C. M. Duarte, C. E. Lovelock, W. H. Schlesinger, B. R. Silliman, A blueprint for blue carbon: Toward an improved understanding of the role of vegetated coastal habitats in sequestering CO_2. *Front. Ecol. Environ.* **9**, 552–560 (2011).
6. C. M. Duarte, I. J. Losada, I. E. Hendriks, I. Mazarrasa, N. Marbà, The role of coastal plant communities for climate change mitigation and adaptation. *Nat. Clim. Chang.* **3**, 961–968 (2013).
7. C. Nellemann, E. Corcoran, C. M. Duarte, L. Valdés, C. De Young, L. Fonseca, G. Grimsditch, *Blue Carbon. A Rapid Response Assessment* (United Nations Environment Programme, GRID-Arendal, 2009).
8. C. M. Duarte, J. J. Middelburg, N. Caraco, Major role of marine vegetation on the oceanic carbon cycle. *Biogeosciences* **2**, 1–8 (2005).
9. L. Pendleton, D. C. Donato, B. C. Murray, S. Crooks, W. A. Jenkins, S. Sifleet, C. Craft, J. W. Fourqurean, J. B. Kauffman, N. Marbà, P. Megonigal, E. Pidgeon, D. Herr, D. Gordon, A. Baldera, Estimating global "blue carbon" emissions from conversion and degradation of vegetated coastal ecosystems. *PLOS ONE* **7**, e43542 (2012).
10. D. C. Donato, J. B. Kauffman, D. Murdiyarso, S. Kurnianto, M. Stidham, M. Kanninen, Mangroves among the most carbon-rich forests in the tropics. *Nat. Geosci.* **4**, 293–297 (2011).
11. D. M. Alongi, Carbon cycling and storage in mangrove forests. *Annu. Rev. Mar. Sci.* **6**, 195–219 (2014).
12. S. Bouillon, A. V. Borges, E. Castañeda-Moya, K. Diele, T. Dittmar, N. C. Duke, E. Kristensen, S. Y. Lee, C. Marchand, J. J. Middelburg, V. H. Rivera-Monroy, T. J. Smith III, R. R. Twilley, Mangrove production and carbon sinks: A revision of global budget estimates. *Global Biogeochem. Cycles* **22**, GB2013 (2008).
13. D. M. Alongi, S. K. Mukhopadhyay, Contribution of mangroves to coastal carbon cycling in low latitude seas. *Agric. For. Meteorol.* **213**, 266–272 (2015).
14. J. A. Rosentreter, D. T. Maher, D. V. Erler, R. Murray, B. D. Eyre, Seasonal and temporal CO_2 dynamics in three tropical mangrove creeks—A revision of global mangrove CO_2 emissions. *Geochim. Cosmochim. Acta* **222**, 729–745 (2018).
15. J. L. Breithaupt, J. M. Smoak, T. J. Smith, C. J. Sanders, A. Hoare, Organic carbon burial rates in mangrove sediments: Strengthening the global budget. *Global Biogeochem. Cycles* **26**, 1–11 (2012).
16. R. Conrad, Control of hydrogen to methane production and control of hydrogen concentrations in methanogenic soils and sediments. *FEMS Microbiol. Ecol.* **28**, 193–202 (1999).
17. R. Conrad, Quantification of methanogenic pathways using stable carbon isotopic signatures: A review and a proposal. *Org. Geochem.* **36**, 739–752 (2005).
18. R. R. Twilley, R. H. Chen, T. Hargis, Carbon sinks in mangroves and their implications to carbon budget of tropical coastal ecosystems. *Water Air Soil Pollut.* **64**, 265–288 (1992).
19. D. Sotomayor, J. F. Corredor, J. M. Morell, Methane flux from mangrove sediments along the southwestern coast of Puerto Rico. *Estuaries* **17**, 140–147 (1994).
20. E. Kristensen, M. R. Flindt, S. Ulomi, A. V. Borges, G. Abril, S. Bouillon, Emission of CO_2 and CH_4 to the atmosphere by sediments and open waters in two Tanzanian mangrove forests. *Mar. Ecol. Prog. Ser.* **370**, 53–67 (2008).
21. R. Purvaja, R. Ramesh, P. Frenzel, Plant-mediated methane emission from an Indian mangrove. *Glob. Chang. Biol.* **10**, 1825–1834 (2004).
22. J. Barnes, R. Ramesh, R. Purvaja, A. Nirmal Rajkumar, B. Senthil Kumar, K. Krithika, K. Ravichandran, G. Uher, R. Upstill-Goddard, Tidal dynamics and rainfall control N_2O and CH_4 emissions from a pristine mangrove creek. *Geophys. Res. Lett.* **33**, L15405 (2006).
23. M. Call, D. T. Maher, I. R. Santos, S. Ruiz-Halpern, P. Mangion, C. J. Sanders, D. V. Erler, J. M. Oakes, J. Rosentreter, R. Murray, B. D. Eyre, Spatial and temporal variability of carbon dioxide and methane fluxes over semi-diurnal and spring–neap–spring timescales in a mangrove creek. *Geochim. Cosmochim. Acta* **150**, 211–225 (2015).
24. N. Linto, J. Barnes, R. Ramachandran, J. Divia, P. Ramachandran, R. C. Upstill-Goddard, Carbon dioxide and methane emissions from mangrove-associated waters of the Andaman Islands, Bay of Bengal. *Estuaries Coasts* **37**, 381–398 (2014).
25. C. Giri, E. Ochieng, L. L. Tieszen, Z. Zhu, A. Singh, T. Loveland, J. Masek, N. Duke, Status and distribution of mangrove forests of the world using earth observation satellite data. *Glob. Ecol. Biogeogr.* **20**, 154–159 (2011).
26. D. T. Ho, N. Coffineau, B. Hickman, N. Chow, T. Koffman, P. Schlosser, Influence of current velocity and wind speed on air-water gas exchange in a mangrove estuary. *Geophys. Res. Lett.* **43**, 3813–3821 (2016).
27. J. A. Rosentreter, D. T. Maher, D. T. Ho, M. Call, J. G. Barr, B. D. Eyre, Spatial and temporal variability of CO_2 and CH_4 gas transfer velocities and quantification of the CH_4 microbubble flux in mangrove dominated estuaries. *Limnol. Oceanogr.* **62**, 561–578 (2017).
28. M.-J. Gonsalves, C. E. G. Fernandes, S. O. Fernandes, D. L. Kirchman, P. A. L. Bharathi, Effects of composition of labile organic matter on biogenic production of methane in the coastal sediments of the Arabian Sea. *Environ. Monit. Assess.* **182**, 385–395 (2011).
29. A. R. C. Ovalle, C. E. Rezende, L. D. Lacerda, C. A. R. Silva, Factors affecting the hydrochemistry of a mangrove tidal creek, Sepetiba Bay, Brazil. *Estuar. Coast. Shelf Sci.* **31**, 639–650 (1990).
30. D. T. Maher, I. R. Santos, J. Gleeson, B. D. Eyre, Groundwater-derived dissolved inorganic and organic carbon exports from a mangrove tidal creek : The missing mangrove carbon sink? *Limnol. Oceanogr.* **58**, 475–488 (2013).
31. R. J. Lara, T. Dittmar, Nutrient dynamics in a mangrove creek (North Brazil) during the dry season. *Mangroves Salt Marshes* **3**, 185–195 (1999).
32. T. Enns, P. F. Scholander, E. D. Bradstreet, The effect of hydrostatic pressure on gases dissolved in water. *J. Phys. Chem.* **69**, 389–391 (1965).
33. M. A. De Angelis, M. I. Scranton, Fate of methane in the Hudson River and estuary. *Global Biogeochem. Cycles* **7**, 509–523 (1993).
34. A. Maeck, H. Hofmann, A. Lorke, Pumping methane out of aquatic sediments—Ebullition forcing mechanisms in an impounded river. *Biogeosciences* **11**, 2925–2938 (2014).
35. M. E. Repo, J. T. Huttunen, A. V. Naumov, A. V. Chichulin, E. D. Lapshina, W. Bleuten, P. J. Martikainen, Release of CO_2 and CH_4 from small wetland lakes in western Siberia. *Tellus B Chem. Phys. Meteorol.* **59**, 788–796 (2007).
36. C. J. Sanders, D. T. Maher, D. R. Tait, D. Williams, C. Holloway, J. Z. Sippo, I. R. Santos, Are global mangrove carbon stocks driven by rainfall? *J. Geophys. Res.* **121**, 2600–2609 (2016).
37. P. Saenger, S. C. Snedaker, Pantropieal trends in mangrove above-ground biomass and annual litterfall. *Oecologia* **96**, 293–299 (1993).
38. X. Ouyang, S. Y. Lee, R. M. Connolly, The role of root decomposition in global mangrove and saltmarsh carbon budgets. *Earth Sci. Rev.* **166**, 53–63 (2017).
39. C. J. Sanders, J. M. Smoak, A. S. Naidu, L. M. Sanders, S. R. Patchineelam, Organic carbon burial in a mangrove forest, margin and intertidal mud flat. *Estuar. Coast. Shelf Sci.* **90**, 168–172 (2010).
40. D. T. Maher, K. Cowley, I. R. Santos, P. Macklin, B. D. Eyre, Methane and carbon dioxide dynamics in a subtropical estuary over a diel cycle: Insights from automated in situ radioactive and stable isotope measurements. *Mar. Chem.* **168**, 69–79 (2015).
41. S. Bouillon, S. Bouillon, J. J. Middelburg, F. Dehairs, A. V. Borges, G. Abril, M. R. Flindt, S. Ulomi, E. Kristensen, Importance of intertidal sediment processes and porewater exchange on the water column biogeochemistry in a pristine mangrove creek (Ras Dege, Tanzania). *Biogeosciences* **4**, 311–322 (2007).
42. N. C. Duke, M. C. Ball, J. C. Ellison, Factors influencing biodiversity and distributional gradients in mangroves. *Glob. Ecol. Biogeogr. Lett.* **7**, 27–47 (1998).
43. D. Murdiyarso, J. Purbopuspito, J. Boone Kauffman, M. W. Warren, S. D. Sasmito, D. C. Donato, S. Manuri, H. Krisnawati, S. Taberima, S. Kurnianto, The potential of Indonesian mangrove forests for global climate change mitigation. *Nat. Clim. Chang.* **5**, 1089–1092 (2015).
44. C. M. Duarte, Reviews and syntheses: Hidden forests, the role of vegetated coastal habitats in the ocean carbon budget. *Biogeosciences* **14**, 301–310 (2017).
45. I. Valiela, J. L. Bowen, J. K. York, Mangrove forests: One of the world's threatened major tropical environments. *Bioscience* **51**, 807 (2001).
46. N. C. Duke, J. M. Kovacs, A. D. Griffiths, L. Preece, D. J. E. Hill, P. van Oosterzee, J. Mackenzie, H. S. Morning, D. Burrows, Large-scale dieback of mangroves in Australia's Gulf of Carpentaria: A severe ecosystem response, coincidental with an unusually extreme weather event. *Mar. Freshwater Res.* **68**, 1816–1829 (2017).
47. D. M. Alongi, Present state and future of the world's mangrove forests. *Environ. Conserv.* **29**, 331–349 (2002).
48. N. C. Duke, J.-O. Meynecke, S. Dittmann, A. M. Ellison, K. Anger, U. Berger, S. Cannicci, K. Diele, K. C. Ewel, C. D. Field, N. Koedam, S. Y. Lee, C. Marchand, I. Nordhaus, F. Dahdouh-Guebas, A world without mangroves? *Science* **317**, 41–43 (2007).
49. M. D. Spalding, M. Kainuma, L. Collins, *World Atlas of Mangroves* (Earthscan, 2010).
50. K. Rogers, N. Saintilan, H. Heijnis, Mangrove encroachment of salt marsh in Western Port Bay, Victoria: The role of sedimentation, subsidence, and sea level rise. *Estuaries* **28**, 551–559 (2005).
51. D. F. McGinnis, G. Kirillin, K. W. Tang, S. Flury, P. Bodmer, C. Engelhardt, P. Casper, H. P. Grossart, Enhancing surface methane fluxes from an oligotrophic lake: Exploring the microbubble hypothesis. *Environ. Sci. Technol.* **49**, 873–880 (2015).
52. Y. T. Prairie, P. A. del Giorgio, A new pathway of freshwater methane emissions and the putative importance of microbubbles. *Inland Waters* **3**, 311–320 (2013).
53. R. Wanninkhof, Relationship between wind speed and gas exchange over the ocean revisited. *Limnol. Oceanogr. Methods* **12**, 351–362 (2014).
54. P. A. Raymond, J. J. Cole, Gas exchange in rivers and estuaries: Choosing a gas transfer velocity. *Estuaries* **24**, 312–317 (2001).

55. A. V. Borges, J.-P. Vanderborght, L.-S. Schiettecatte, F. Gazeau, S. Ferrón-Smith, B. Delille, M. Frankignoulle, Variability of the gas transfer velocity of CO_2 in a macrotidal estuary (the Scheldt). *Estuaries* **27**, 593–603 (2004).
56. M. J. Prather, C. D. Holmes, J. Hsu, Reactive greenhouse gas scenarios: Systematic exploration of uncertainties and the role of atmospheric chemistry. *Geophys. Res. Lett.* **39**, 6–10 (2012).
57. B. D. Eyre, A first-order nutrient budget for the tropical Moresby estuary and catchment, North Queensland, Australia. *J. Coast. Res.* **11**, 717–732 (1995).
58. B. D. Eyre, A. J. P. Ferguson, A. Webb, D. Maher, J. M. Oakes, Metabolism of different benthic habitats and their contribution to the carbon budget of a shallow oligotrophic sub-tropical coastal system (southern Moreton Bay, Australia). *Biogeochemistry* **102**, 87–110 (2011).
59. S. Lekphet, S. Nitisoravut, S. Adsavakulchai, Estimating methane emissions from mangrove area in Ranong Province, Thailand. *Songklanakarin J. Sci. Technol.* **27**, 153–163 (2005).
60. S. J. Livesley, S. M. Andrusiak, Temperate mangrove and salt marsh sediments are a small methane and nitrous oxide source but important carbon store. *Estuar. Coast. Shelf Sci.* **97**, 19–27 (2012).
61. J. Kreuzwieser, J. Buchholz, H. Rennenberg, Emission of methane and nitrous oxide by Australian mangrove ecosystem. *Plant Biol.* **5**, 423–431 (2003).
62. D. E. Allen, R. C. Dalal, H. Rennenberg, R. L. Meyer, S. Reeves, S. Schmidt, Spatial and temporal variation of nitrous oxide and methane flux between subtropical mangrove sediments and the atmosphere. *Soil Biol. Biochem.* **39**, 622–631 (2007).
63. D. Allen, R. C. Dalal, H. Rennenberg, S. Schmidt, Seasonal variation in nitrous oxide and methane emissions from subtropical estuary and coastal mangrove sediments, Australia. *Plant Biol.* **13**, 126–133 (2010).
64. G. Chen, B. Chen, D. Yu, N. F. Y. Tam, Y. Ye, S. Chen, Soil greenhouse gas emissions reduce the contribution of mangrove plants to the atmospheric cooling effect. *Environ. Res. Lett.* **11**, 124019 (2016).
65. D. M. Alongi, J. Pfitzner, L. A. Trott, F. Tirendi, P. Dixon, D. W. Klumpp, Rapid sediment accumulation and microbial mineralization in forests of the mangrove *Kandelia candel* in the Jiulongjiang Estuary, China. *Estuar. Coast. Shelf Sci.* **63**, 605–618 (2005).
66. G. C. Chen, N. F. Y. Tam, Y. Ye, Summer fluxes of atmospheric greenhouse gases N_2O, CH_4 and CO_2 from mangrove soil in South China. *Sci. Total Environ.* **408**, 2761–2767 (2010).
67. M. K. Dutta, T. S. Bianchi, S. K. Mukhopadhyay, Mangrove methane biogeochemistry in the Indian Sundarbans: A proposed budget. *Front. Mar. Sci.* **4**, 187 (2017).
68. R. Chauhan, A. L. Ramanathan, T. K. Adhya, Assessment of methane and nitrous oxide flux from mangroves along Eastern coast of India. *Geofluids* **8**, 321–332 (2008).
69. R. Chauhan, A. Datta, A. Ramanathan, T. K. Adhya, Factors influencing spatio-temporal variation of methane and nitrous oxide emission from a tropical mangrove of eastern coast of India. *Atmos. Environ.* **107**, 95–106 (2015).
70. C. Y. Lu, Y. S. Wong, N. F. Y. Tam, Y. Ye, P. Lin, Methane flux and production from sediments of a mangrove wetland on Hainan Island, China. *Mangroves Salt Marshes* **3**, 41–49 (1999).
71. D. M. Alongi, F. Tirendi, P. Dixon, L. A. Trott, G. J. Brunskill, Mineralization of organic matter in intertidal sediments of a tropical semi-enclosed delta. *Estuar. Coast. Shelf Sci.* **48**, 451–467 (1999).
72. T. J. Lyimo, A. Pol, H. J. M. Op den Camp, Methane emission, sulphide concentration and redox potential profiles in Mtoni mangrove sediment, Tanzania. *Western Indian Ocean Journal of Marine Science* **1**, 71–80 (2002).
73. D. M. Alongi, A. Sasekumar, V. C. Chong, J. Pfitzner, L. A. Trott, F. Tirendi, P. Dixon, G. J. Brunskilla, Sediment accumulation and organic material flux in a managed mangrove ecosystem: Estimates of land–ocean–atmosphere exchange in peninsular Malaysia. *Mar. Geol.* **208**, 383–402 (2004).
74. T. S. Bianchi, M. A. Allison, J. Zhao, X. Li, R. S. Comeaux, R. A. Feagin, R. Wasantha Kulawardhana, Historical reconstruction of mangrove expansion in the Gulf of Mexico: Linking climate change with carbon sequestration in coastal wetlands. *Estuar. Coast. Shelf Sci.* **119**, 7–16 (2013).
75. C. J. Sanders, I. R. Santos, D. T. Maher, J. L. Breithaupt, J. M. Smoak, M. Ketterer, M. Call, L. Sanders, B. D. Eyre, Examining $^{239+240}$Pu, ^{210}Pb and historical events to determine carbon, nitrogen and phosphorus burial in mangrove sediments of Moreton Bay, Australia. *J. Environ. Radioact.* **151**, 623–629 (2016).
76. J. C. Lynch, J. R. Meriwether, B. A. McKee, F. Vera-Herrera, R. R. Twilley, Recent accretion in mangrove ecosystems based on ^{137}Cs and ^{210}Pb. *Estuaries* **12**, 284–299 (1989).
77. G. L. Chmura, S. C. Anisfeld, D. R. Cahoon, J. C. Lynch, Global carbon sequestration in tidal, saline wetland soils. *Global Biogeochem. Cycles* **17**, 1111 (2003).
78. D. A. Marchio, M. Savarese, B. Bovard, W. J. Mitsch, Carbon sequestration and sedimentation in mangrove swamps influenced by hydrogeomorphic conditions and urbanization in Southwest Florida. *Forests* **7**, 1–18 (2016).
79. C. J. Sanders, J. M. Smoak, M. N. Waters, L. M. Sanders, N. Brandini, S. R. Patchineelam, Organic matter content and particle size modifications in mangrove sediments as responses to sea level rise. *Mar. Environ. Res.* **77**, 150–155 (2012).
80. C. J. Sanders, J. M. Smoak, L. M. Sanders, A. Sathy Naidu, S. R. Patchineelam, Organic carbon accumulation in Brazilian mangal sediments. *J. South Am. Earth Sci.* **30**, 189–192 (2010).
81. J. M. Smoak, J. L. Breithaupt, T. J. Smith, C. J. Sanders, Sediment accretion and organic carbon burial relative to sea-level rise and storm events in two mangrove forests in Everglades National Park. *Catena* **104**, 58–66 (2013).
82. J. L. Breithaupt, J. M. Smoak, T. J. Smith III, C. J. Sanders, Temporal variability of carbon and nutrient burial, sediment accretion, and mass accumulation over the past century in a carbonate platform mangrove forest of the Florida Everglades. *J. Geophys. Res. Biogeosci.* **119**, 2032–2048 (2014).
83. C. J. Sanders, J. M. Smoak, A. S. Naidu, S. R. Patchineelam, Recent sediment accumulation in a mangrove forest and its relevance to local sea-level rise (Ilha Grande, Brazil). *J. Coast. Res.* **24**, 533–536 (2008).
84. C. J. Sanders, J. M. Smoak, A. S. Naidu, D. R. Araripe, L. M. Sanders, S. R. Patchineelam, Mangrove forest sedimentation and its reference to sea level rise, Cananeia, Brazil. *Environ. Earth Sci.* **60**, 1291–1301 (2010).
85. J. C. Callaway, R. D. Delaune, W. H. Patrick Jr., Sediment accretion rates from four coastal wetlands along the Gulf of Mexico. *J. Coast. Res.* **13**, 181–191 (1997).
86. Y. Tateda, D. D. Nhan, G. Wattayakorn, H. Toriumi, Preliminary evaluation of organic carbon sedimentation rates in Asian mangrove coastal ecosystems estimated by ^{210}Pb chronology. *Radioprotection* **40**, 527–532 (2005).
87. M. E. Gonneea, A. Paytan, J. A. Herrera-Silveira, Tracing organic matter sources and carbon burial in mangrove sediments over the past 160 years. *Estuar. Coast. Shelf Sci.* **61**, 211–227 (2004).
88. G. J. Brunskill, I. Zagorskis, J. Pfitzner, Carbon burial rates in sediments and a carbon mass balance for the Herbert River region of the Great Barrier Reef continental shelf, North Queensland, Australia. *Estuar. Coast. Shelf Sci.* **54**, 677–700 (2002).
89. D. M. Alongi, G. Wattayakorn, J. Pfitzner, F. Tirendi, I. Zagorskis, G. J. Brunskill, A. Davidson, B. F. Clough, Organic carbon accumulation and metabolic pathways in sediments of mangrove forests in southern Thailand. *Mar. Geol.* **179**, 85–103 (2001).
90. G. J. Brunskill, I. Zagorskis, J. Pfitzner, J. Ellison, Sediment and trace element depositional history from the Ajkwa River estuarine mangroves of Irian Jaya (West Papua), Indonesia. *Cont. Shelf Res.* **24**, 2535–2551 (2004).
91. M. I. Bird, L. K. Fifield, S. Chua, B. Goh, Calculating sediment compaction for radiocarbon dating of intertidal sediments. *Radiocarbon* **46**, 421–435 (2004).

Acknowledgments: We would like to thank M. Call and A. McMahon for their fieldwork assistance. **Funding:** This project was funded by the Great Barrier Reef Foundation's Resilient Coral Reefs Successfully Adapting to Climate Change research and development program in collaboration with the Australian Government and by Australian Research Council grants DE150100581, DP160100248, and LP150100519. This work was inspired by the Commonwealth Scientific and Industrial Research Organisation Flagship Marine and Coastal Carbon Biogeochemical Cluster (Coastal Carbon Cluster). **Author contributions:** J.A.R. contributed to the experimental design, did the field work and data analysis, and wrote most of the manuscript. B.D.E. conceived the project, contributed to the experimental design, assisted with the data analysis, and wrote parts of the manuscript. D.T.M. contributed to the experimental design, assisted with field work and data analysis, and wrote parts of the manuscript. D.V.E. and R.H.M. assisted with the field work and data analysis. All authors reviewed and edited the manuscript. **Competing interests:** The authors declare that they have no competing interests. **Data and materials availability:** All data needed to evaluate the conclusions in the paper are present in the paper and/or the Supplementary Materials. Additional data related to this paper may be requested from the authors.

Submitted 27 July 2017
Accepted 30 March 2018
Published 13 June 2018
10.1126/sciadv.aao4985

Citation: J. A. Rosentreter, D. T. Maher, D. V. Erler, R. H. Murray, B. D. Eyre, Methane emissions partially offset "blue carbon" burial in mangroves. *Sci. Adv.* **4**, eaao4985 (2018).

Methane emissions partially offset "blue carbon" burial in mangroves

Judith A. Rosentreter, Damien T. Maher, Dirk V. Erler, Rachel H. Murray and Bradley D. Eyre

Sci Adv **4** (6), eaao4985.
DOI: 10.1126/sciadv.aao4985